

Precision Measurement of $R = \sigma_L/\sigma_T$ and F_2 in Deep-Inelastic Electron Scattering

S. Dasu,⁽¹⁾ P. de Barbaro,⁽¹⁾ A. Bodek,⁽¹⁾ H. Harada,⁽¹⁾ M. W. Krasny,⁽¹⁾ K. Lang,⁽¹⁾ E. M. Riordan,⁽¹⁾ R. Arnold,⁽²⁾ D. Benton,⁽²⁾ P. Bosted,⁽²⁾ L. Clogher,⁽²⁾ G. deChambrier,⁽²⁾ A. Lung,⁽²⁾ S. E. Rock,⁽²⁾ Z. M. Szalata,⁽²⁾ R. C. Walker,⁽³⁾ B. W. Filippone,⁽³⁾ J. Jourdan,⁽³⁾ R. Milner,⁽³⁾ R. McKeown,⁽³⁾ D. Potterveld,⁽³⁾ A. Para,⁽⁴⁾ F. Dietrich,⁽⁵⁾ K. Van Bibber,⁽⁵⁾ J. Button-Shafer,⁽⁶⁾ B. Debebe,⁽⁶⁾ R. S. Hicks,⁽⁶⁾ R. Gearhart,⁽⁷⁾ L. W. Whitlow,⁽⁸⁾ and J. Alster⁽⁹⁾

⁽¹⁾University of Rochester, Rochester, New York 14627

⁽²⁾The American University, Washington, D.C. 20016

⁽³⁾California Institute of Technology, Pasadena, California 91125

⁽⁴⁾Fermi National Accelerator Laboratory, Batavia, Illinois 60510

⁽⁵⁾Lawrence Livermore National Laboratory, Livermore, California 94550

⁽⁶⁾University of Massachusetts, Amherst, Massachusetts 01003

⁽⁷⁾Stanford Linear Accelerator Center, Stanford, California 94305

⁽⁸⁾Stanford University, Stanford, California 94305

⁽⁹⁾University of Tel-Aviv, Ramat Aviv, Tel-Aviv 69978, Israel

(Received 20 May 1988)

We report new results on a precision measurement of the ratio $R = \sigma_L/\sigma_T$ and the structure function F_2 for deep-inelastic electron-nucleon scattering in the kinematic range $0.2 \leq x \leq 0.5$ and $1 \leq Q^2 \leq 10$ (GeV/c)². Our results show, for the first time, a clear falloff of R with increasing Q^2 . Our R and F_2 results are in good agreement with QCD predictions only when corrections for target-mass effects are included.

PACS numbers: 13.60.Hb, 12.38.Qk, 25.30.Fj

The ratio $R = \sigma_L/\sigma_T$ of the longitudinal (σ_L) and transverse (σ_T) virtual-photon absorption cross sections measured in deep-inelastic lepton-nucleon scattering is a sensitive measure of the spin and the transverse momentum of the nucleon constituents. In the naive parton model with spin- $\frac{1}{2}$ partons, R is expected to be small, and to decrease rapidly with increasing momentum transfer, Q^2 . With spin-0 partons, R should be large and increase with Q^2 . Previous measurements¹⁻³ of R at the Stanford Linear Accelerator Center (SLAC) indicated that scattering from spin- $\frac{1}{2}$ constituents (e.g., quarks) dominates. However, the values of R were larger than expected, consistent with a constant value of 0.2. The measurement errors on those results left room for speculation about small admixtures of spin-0 constituents in nucleons⁴ (e.g., tightly bound diquarks) and about unexpectedly large primordial transverse momentum for quarks.

Experiments² in the SLAC Q^2 range [$1 \leq Q^2 \leq 20$ (GeV/c)²] have also indicated deviations from the scal-

ing of the structure functions F_1 and F_2 . In quantum chromodynamics (QCD), logarithmic scaling violations⁵ occur because of quark-gluon interactions. In addition, target-mass⁶ and dynamical higher-twist⁷ (nonperturbative effects due to binding of quarks in a nucleon) effects yield power-law violations of scaling. These effects lead to nonzero contributions to R which decrease with increasing Q^2 .

Since the quality of the previous data was inadequate to test such predictions for R , we have made precision measurements of deep-inelastic electron-nucleon scattering cross sections from D, Fe, and Au targets, with particular emphasis on the extraction of the ratio R , and the structure functions F_1 and F_2 . Studies of the difference $R^{\text{Fe}} - R^{\text{D}}$ and the ratio $F_2^{\text{Fe}}/F_2^{\text{D}}$ were presented earlier.⁸ Here we report our results on the kinematic variation of R and F_2 .

The differential cross section for scattering of an unpolarized charged lepton with an incident energy E , final energy E' , and scattering angle θ can be written in terms of the structure functions F_1 and F_2 as

$$\begin{aligned} \sigma &= \frac{d^2\sigma}{d\Omega dE'}(E, E', \theta) = \frac{4a^2 E'^2}{Q^4} \cos^2(\theta/2) [F_2(x, Q^2)/\nu + 2 \tan^2(\theta/2) F_1(x, Q^2)/M] \\ &= \Gamma \sigma_T(x, Q^2) [1 + \epsilon R(x, Q^2)], \end{aligned} \quad (1)$$

where a is the fine-structure constant, M is the nucleon mass, $\nu = E - E'$ is energy of the virtual photon which mediates the interaction, $Q^2 = 4EE' \sin^2(\theta/2)$ is the invariant four-momentum transfer squared, and $x = Q^2/2M\nu$ is a measure of the longitudinal momentum carried by the struck partons. In Eq. (1) the differential cross

section is also related to $R(x, Q^2)$, with

$$\Gamma = \frac{\alpha}{4\pi^2} \frac{(2M\nu - Q^2)E'}{Q^2 M E} \frac{1}{1 - \epsilon},$$

and

$$\epsilon = [1 + 2(1 + v^2/Q^2)\tan^2(\theta/2)]^{-1}$$

representing the virtual-photon flux and polarization, respectively.

The SLAC electron beams and the 8-GeV spectrometer facility² were used to measure cross sections accurate to $\pm 1\%$ in the kinematic range $0.2 \leq x \leq 0.5$ and $1 \leq Q^2 \leq 10$ (GeV/c)² at up to five different values of ϵ (with a typical range of 0.35). Extensive efforts were made in this experiment to reduce systematic errors (summarized in Table I). Systematic effects that can vary with ϵ are especially relevant for the measurement of R . Effects due to beam flux, target density, and background contamination were described earlier.⁸ The spectrometer acceptance in the range $|\Delta p/p| < 3.5\%$, $|\Delta\theta| < 6$ mrad, and $|\Delta\phi| < 28$ mrad, was studied as a function of angle and momentum setting. The change of acceptance with angle for the 20-cm D target was determined to be less than 0.4% with use of a Monte Carlo simulation of spectrometer optics. The momentum dependence of the acceptance ($< 0.3\%$), and the absolute value of the momentum setting ($\pm 0.05\%$) of the spectrometer were studied with a floating-wire technique. Detailed surveys of the spectrometer, targets, and beam line were done before and after the experiment. The absolute error in spectrometer angle was $\pm 0.003^\circ$, with a $\pm 0.0015^\circ$ uncertainty in the reproducibility. Measured elastic-peak positions⁹ were used to determine the uncertainty in the incident energy to $\pm 0.1\%$.

Radiative corrections were calculated with use of the "exact" prescription of Akhundov, Bardin, and Shumeiko¹⁰ (ABS) with additional "external" corrections (due to the straggling of electrons in the target material) calculated in the complete formalism of Mo and Tsai.^{8,11} The "internal" corrections obtained with use of the ABS formalism agreed to better than 1% for each (x, Q^2, ϵ) point with an improved version of the "exact" formalism of Mo and Tsai.¹² In addition, the corrections calculated

TABLE I. Typical systematic errors on σ and R .

Source	Uncertainty	Error (\pm) in	
		σ	R
Beam steering	0.003°	0.1%	0.005
Incident energy	0.1%	0.3%	0.014
Charge measurement	0.3%	0.3%	0.014
Target density	0.2%	0.2%	0.009
Acceptance vs θ	0.1%	0.1%	0.005
Acceptance vs p	0.1%	0.1%	0.005
e^+/e^- background	0.1%	0.1%	0.005
Scattered energy	0.05%	0.1%	0.005
Spectrometer angle	0.002°	0.1%	0.005
Detector efficiency	0.1%	0.1%	0.005
Total point to point		0.5%	0.025
Radiative corrections	1.0%	1.0%	0.030

with different parametrizations of structure functions agreed to better than $\pm 0.2\%$. The ABS approach with fits to previous SLAC data² on F_2 was used for our final results, since it is based on a better theoretical formalism. This approach has also been used in recent neutrino¹³ and muon¹⁴ experiments.

The values of R , F_1 , and F_2 were extracted from cross sections measured at various values of ϵ at fixed (x, Q^2) by our making linear fits, weighted by the statistical and point-to-point systematic uncertainty, to σ/Γ vs ϵ [see Eq. (1)]. The average χ^2/N_{DF} for these fits is 0.7, indicating that the estimate of systematic uncertainty is conservative. R values are insensitive to the absolute normalization of beam flux, target length, radiative corrections, and spectrometer acceptance.

The results for R obtained for all (x, Q^2) points and targets are shown in Table II. Since the differences $R^A - R^D$ are consistent with zero,⁸ the results plotted in Fig. 1 represent averages over various targets at the same x and Q^2 . Our results have small errors [see Fig. 1(a)] compared to previous SLAC experiments^{2,3} (E49, E87, and E89) because (a) our cross sections were measured to better than $\pm 1\%$ statistical accuracy with large ϵ separation, (b) uncertainties in radiative corrections were reduced to the $\pm 1\%$ level, and (c) a single spectrometer with well determined acceptance was used.

TABLE II. Values of R for each (x, Q^2) point and target are tabulated separately with statistical and systematic errors. D and Fe(2) targets are of 2.6% radiation lengths (r.l.) each, whereas Au and Fe(6) are of 6% r.l. Values of χ^2 per degree of freedom for the two-parameter fits are also shown.

Target	x	Q^2 [(GeV/c) ²]	$\Delta\epsilon$	$R = \sigma_L/\sigma_T$			χ^2/N_{DF}
				Value	Stat	Syst	
D	0.20	1.0	0.36	0.348	0.039	0.040	1.8/3
D	0.20	1.5	0.32	0.275	0.041	0.041	5.1/3
D	0.20	2.5	0.37	0.100	0.047	0.039	0.1/1
D	0.20	5.0	0.25	0.198	0.054	0.047	0.8/2
D	0.35	1.5	0.30	0.296	0.050	0.046	0.6/3
D	0.35	2.5	0.36	0.154	0.033	0.038	1.8/3
D	0.35	5.0	0.33	0.126	0.037	0.039	1.0/2
D	0.50	2.5	0.51	0.199	0.025	0.034	2.1/3
D	0.50	5.0	0.46	0.104	0.028	0.036	1.4/2
D	0.50	7.5	0.37	0.155	0.061	0.039	∞/0
D	0.50	10.0	0.35	0.047	0.038	0.038	0.0/1
Fe(2)	0.20	1.0	0.36	0.323	0.042	0.040	0.6/3
Fe(2)	0.50	2.5	0.51	0.221	0.051	0.035	∞/0
Fe(6)	0.20	1.0	0.36	0.270	0.041	0.038	5.1/3
Fe(6)	0.20	1.5	0.32	0.147	0.037	0.038	1.5/3
Fe(6)	0.20	2.5	0.37	0.247	0.058	0.040	1.3/1
Fe(6)	0.35	1.5	0.30	0.344	0.062	0.046	3.3/3
Fe(6)	0.35	2.5	0.36	0.255	0.044	0.038	3.3/3
Fe(6)	0.35	5.0	0.33	0.150	0.045	0.040	0.2/2
Fe(6)	0.50	2.5	0.51	0.220	0.028	0.034	2.1/3
Fe(6)	0.50	5.0	0.46	0.080	0.041	0.035	0.2/2
Au	0.20	1.0	0.36	0.322	0.043	0.041	0.9/3

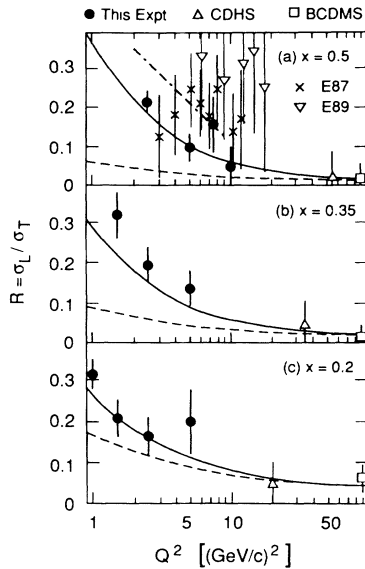


FIG. 1. The values of R at (a) $x=0.5$, (b) $x=0.35$, and (c) $x=0.2$ are plotted vs Q^2 , with statistical and systematic errors added in quadrature. Predictions from perturbative QCD (quark-gluon interaction effects, the dashed curve), QCD with target-mass effects (solid curve), Ekelin and Fredriksson diquark model (dot-dashed curve), and earlier data from experiments E87 and E89 at SLAC, and CDHS (ν -Fe), and BCDMS (μ -C/H) at CERN are also plotted.

Our results at $x=0.2, 0.35$, and 0.5 show a clear falloff of R with increasing Q^2 . The agreement with a constant value of $R=0.2$ is poor ($\chi^2/N_{DF}=34/10$). The high- Q^2 results from the CERN-Dortmund-Heidelberg-Saclay¹³ (CDHS) and Bologna-CERN-Dubna-Munich-Saclay¹⁴ (BCDMS) collaborations for ν -Fe and μ -C/H scattering, respectively, are also plotted. These results reinforce the conclusion that R decreases with increasing Q^2 . Our results at all Q^2 show only a weak x dependence in the range $0.2 \leq x \leq 0.5$.

The values of F_2^D obtained from the fits to σ/Γ vs ϵ are plotted against Q^2 at various x in Fig. 2. These results are preliminary because studies of the absolute normalization (presently known to $\pm 3\%$) are not complete. A weak Q^2 dependence is evident. Earlier SLAC data² are shown for comparison. Note that these early data were radiatively corrected with use of the peaking approximation calculations. Detailed studies of F_2 from all SLAC experiments with our improved radiative corrections and parametrization of R will be reported in a future communication.

In perturbative QCD (to the order α_s) hard gluon bremsstrahlung from quarks and photon-gluon interaction effects yield contributions to the lepton-nucleon scattering cross section.⁵ The leading Q^2 dependence of the structure functions is in α_s , and is therefore logarithmic in Q^2 . The new R data (see Fig. 1) are not in agreement with these calculations¹⁵ ($\chi^2/N_{DF}=98/10$). The

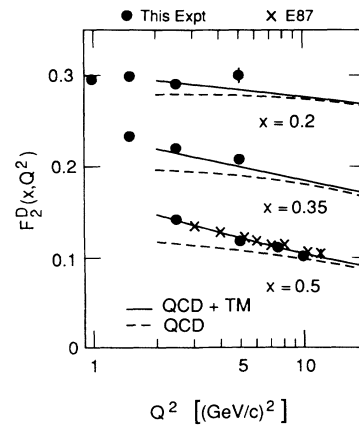


FIG. 2. The values of F_2^D extracted from our data at $x=0.2, 0.35$, and 0.5 are plotted vs Q^2 . Only statistical and point-to-point systematic errors are shown. There is an additional normalization error of $\pm 3\%$. The QCD structure function (dashed curve), and the prediction for F_2 including the target-mass effects (solid curve) are also plotted. Data from SLAC experiment E87 are also plotted at $x=0.5$ for comparison.

scaling violations in F_2 (see Fig. 2) are also not described very well by these QCD interaction effects alone. QCD calculations are not too sensitive to the value of Λ used ($\Lambda=200$ MeV). Target-mass effects⁶ introduce terms proportional to M^2/Q^2 and give large contributions to R and F_2 at small Q^2 and large x . Our data for R and F_2 are in good agreement ($\chi^2/N_{DF}=10/10$) with theory when target-mass effects by Georgi and Politzer⁶ (GP) are added to perturbative QCD. The variation of R with x in the range $0.2 \leq x \leq 0.5$ is weak, in agreement with these predictions. However, the controversy about possible inconsistencies^{7,16} in the original GP target-mass-effect calculations⁶ is yet to be resolved unambiguously.¹⁷ The QCD interactions and target-mass and higher-twist effects can be thought of as giving transverse momentum (k_T) to the quarks. In the naive parton model $R=4\langle k_T^2 \rangle/Q^2$, and the data indicate a $\langle k_T^2 \rangle$ value of 0.10 (GeV/c)² ($\chi^2/N_{DF}=18/10$).

Several authors have speculated⁴ that two of the valence quarks in a nucleon may form a tightly bound spin-0 diquark. The spin-0 diquarks are predicted to give large contributions to R at large x and low Q^2 . Our highest x ($=0.5$) results for R do not favor this possibility. QCD with target-mass effects appears to account for all the Q^2 dependence of R , and therefore speculations⁷ that dynamical higher-twist contributions to R (for $x \leq 0.5$) are large are not supported by our data.

An empirical parametrization of the perturbative QCD calculations of R , with an additional $1/Q^2$ term fitted to our data, is given by

$$R(x, Q^2) = \left[\frac{\alpha(1-x)^\beta}{\ln(Q^2/\Lambda^2)} + \frac{\gamma(1-x)^\delta}{Q^2} \right],$$

where $\alpha=1.11$, $\beta=3.34$, $\gamma=0.11$, $\delta=-1.94$, and $\Lambda=0.2$ GeV/c.

In conclusion, these results show for the first time a clear falloff of R with increasing Q^2 in the range $1 \leq Q^2 \leq 10$ (GeV/c)² for $x=0.2, 0.35$, and 0.5 . R and F_2 are in good agreement with QCD predictions only when corrections for GP target-mass effects are included. The new data do not favor large contributions from diquarks, nonperturbative, and higher-twist effects in our x range.

We acknowledge the support of Dr. B. Richter and the SLAC staff, which was crucial for the success of this experiment. This research was supported by Department of Energy Contracts No. DE-AC02-76ER13065, No. DE-AC02-76ER02853, and No. DE-AC03-76SF00515, and National Science Foundation Grants No. PHY84-10549 and No. PHY85-05682.

¹M. Breidenbach *et al.*, Phys. Rev. Lett. **23**, 930 (1969); G. Miller *et al.*, Phys. Rev. D **5**, 528 (1972).

²E. M. Riordan *et al.*, Phys. Rev. Lett. **33**, 561 (1974); A. Bodek *et al.*, Phys. Rev. D **20**, 1471 (1979) (E49 and E87).

³M. D. Mestayer *et al.*, Phys. Rev. D **27**, 285 (1983) (E89).

⁴L. F. Abbott *et al.*, Phys. Lett. **88B**, 157 (1979); S. Ekelin and S. Fredriksson, Phys. Lett. **162B**, 373 (1985).

⁵G. Altarelli and G. Martinelli, Phys. Lett. **76B**, 89 (1978).

⁶H. Georgi and D. Politzer, Phys. Rev. D **14**, 1829 (1976); R. Barbieri *et al.*, Nucl. Phys. **B117**, 50 (1976); A. De Rújula *et al.*, Ann. Phys. (N.Y.) **103**, 315 (1977); A. Buras *et al.*, Nucl. Phys. **B131**, 308 (1977); O. Nachtmann, Nucl. Phys. **B63**, 237 (1973).

⁷J. L. Miramontes and J. Sanchez Guillen, University of

Santiago de Copostela, Spain, Report No. US/FT-1/88, 1988 (to be published).

⁸S. Dasu *et al.*, Phys. Rev. Lett. **60**, 2591 (1988).

⁹During this experiment elastic-scattering data were also taken to extract the proton electric form factor G_E^p . See R. C. Walker *et al.*, to be published.

¹⁰A. A. Akhundov, D. Yu. Bardin, and N. M. Shumeiko, Yad. Fiz. **26**, 1251 (1977) [Sov. J. Nucl. Phys. **26**, 660 (1977)], and references therein.

¹¹L. W. Mo and Y. S. Tsai, Rev. Mod. Phys. **41**, 205 (1969); Y. S. Tsai, SLAC Report No. SLAC-PUB-848, 1971 (unpublished).

¹²The exact formalism of Mo and Tsai is not explicitly provided in Ref. 11. Our procedure included (a) the addition of μ , τ , and quark loops to vacuum polarization diagram, (b) a correction for multiple soft-photon emission (this was used in the peaking approximation formulas but not in the exact formula A.24 of Tsai, Ref. 11), and (c) the numerical integration of the bremsstrahlung photon angle integral for photon energy less than the cutoff (Δ). See S. Dasu, Ph. D. thesis, University of Rochester, University of Rochester Report No. UR-1059, 1988 (unpublished) for details.

¹³P. Buchholz (CDHS Collaboration), in *Proceedings of the International Europhysics Conference on High Energy Physics, Bari, 1985*, edited by L. Nitti and G. Preparata (European Physical Society, Switzerland, 1986).

¹⁴A. C. Benvenuti *et al.* (BCDMS Collaboration), Phys. Lett. **B 195**, 91 (1987).

¹⁵The input quark distribution fits for these calculations were obtained from the CDHS Collaboration; see B. Vallage, Ph. D. thesis, University de Paris—Sud, 1984 (unpublished). These quark distributions agreed with our data for F_1 , for which the target-mass effects are negligible. See Dasu, Ref. 12.

¹⁶D. J. Gross *et al.*, Phys. Rev. D **15**, 2486 (1977).

¹⁷Dasu, Ref. 12.